TANDEM BLUE-VIOLET QUANTUM WELL InGaN LASERS WITH HIGH-FREQUENCY SELF-PULSATIONS

I. Antohi, S. Rusu, and V. Z. Tronciu

Department of Physics, Technical University of Moldova, Chisinau, MD2004 Republic of Moldova

(Received November 19, 2013)

Abstract

Theoretical investigations have been carried out to study the dynamics of tandem blue–violet lasers. The theoretical results show that self-pulsating operations are possible if one of the regions is adjusted with an external electric circuit. Self-pulsation with high frequencies has been observed in the numerical calculations. We found that features of the external circuit strongly affect the self-pulsation. The effect of device and material parameters on the laser dynamics was also investigated.

1. Introduction

During recent years, blue–violet semiconductor lasers have received much attention because they are promising for high-density optical storage applications [1]. Laser diodes of the blue-violet light operating at a wavelength of 405 nm are necessary to increase the storage capacity of the disc up to 25 GB. In particular, blue–violet lasers are required for BD-systems [2] and for use in medicine, biology, color printers and monitors, etc. In recent years, numerous fabrication methods have been proposed and developed for blue lasers with CW and self-pulsating operations and the lifetime of these lasers has been increased to over 15 000 h. Several groups have reported the CW operation at room temperature using different fabrications methods [3–5]. The phenomenon of self-pulsation (SP) is considered to be the most important for reduction of the feedback noise [6, 7]. Recently, we have reported self-pulsation and excitable behavior for an InGaN laser with a p-type saturable absorber, and SP in the frequency range of 1.6 to 2.9 GHz has been achieved with these lasers [8–11].

In this paper, we focus on the generation of SP in a multi quantum-well (MQW) tandem InGaN laser with an additional controllable section. The purpose of this study is to extend the investigations of [12] and describe the self-pulsating characteristics of an InGaN MQW laser with an SA, which can generate self-pulsations at room temperature. The paper is organized as follows. In Section II, we present the laser structure, model, and equations. In Section III, numerically simulated results of a self-pulsating InGaN laser are shown and we study how the laser and material parameters influence the laser dynamics. Finally, the conclusions are given in Section IV.

2. Model and equations

A sketch of the investigated tandem laser is shown in Fig. 1 and comprises an active main region A coupled to an additional region B. Region B has been introduced to control the feedback that is coming back to the main region. By adjusting switch K, we can optimize the frequency of

self-pulsations. The lengths of two regions are 500 and 50 μm for the A and B regions, respectively. The main current is applied to region A. The contact of region B has an electrical connection that can be broken by means of switch K. If switch K is in position 1, then the current is injected into region B and this region becomes active. For position 2 of switch K, the current is not injected into region B and this region acts as a saturable absorber. In position 3 of switch K, an external circuit is connected and the carriers flow through it due to the diffusion.

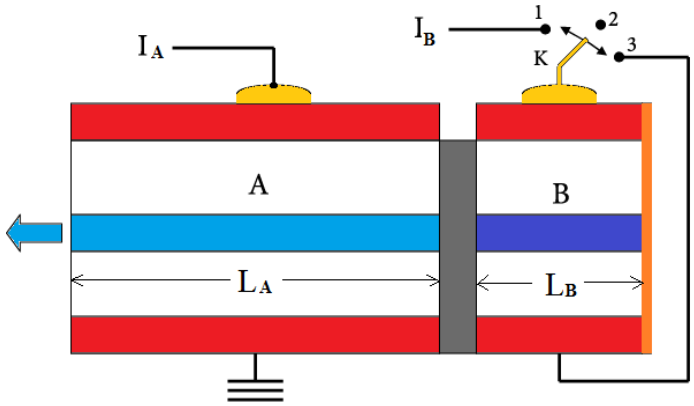

Fig. 1. A schematic diagram of the proposed blue InGaN tandem laser structure.

The theoretical analysis is applied to the structure of the fabricated laser samples [12]. In the present study, the laser dynamics is analyzed in the framework of the single mode model presented in [12]:

$$\frac{dS}{dt}=\left[\frac{L_A}{L}a_A\xi_A(n_A-n_{gA})+\frac{L_B}{L}a_B\xi_B(n_B-n_{gB})-G_{th}\right]S+M\left[a_A\frac{L_A}{L}\xi_A n_A+a_B\frac{L_B}{L}\xi_B n_B\right], \quad (1)$$

$$\frac{dn_A}{dt}=-\frac{a_A}{V_A}\frac{L_A}{L}\mathrm{x}_A(n_A-n_{gA})S-\frac{n_A}{\mathrm{t}_{SA}}+\frac{I_A}{eV_A}, \quad (2)$$

$$\frac{dn_B}{dt}=-\frac{a_B}{V_B}\frac{L_B}{L}\xi_B(n_B-n_{gB})S-\frac{n_B}{\tau_{SB}}+\begin{cases}I_B/eV_B & K-\text{position 1},\\ 0 & K-\text{position 2},\\ -n_B/\tau_T & K-\text{position 3}.\end{cases} \quad (3)$$

where S is the number of photons in the full device, n_A (n_B) is the carriers density in region A (B); L is the length of full device. I_A and I_B are the injected currents into regions A and B, respectively; M is the equivalent total number of the longitudinal modes, which is evaluated from the half width of the linear gain spectrum [13]; τ_T is the effective diffusion lifetime; a_A (a_B) is the differential gain coefficient, ξ_A (ξ_B) is the field confinement factor, which has been calculated for each design and is taken to vary during the pulsations; n_{gA} (n_{gB}) is the transparency carrier density; τ_{sA} (τ_{sB}) is the carrier lifetime. The threshold gain level G_{th} is given by

$$G_{th} = \frac{c}{n_r}\left(k + \frac{1}{2L}\ln\frac{1}{R_f R_b}\right),$$

where R_f and R_b are the reflectivity at the front and the back facets, respectively, and κ is the loss coefficient. The other parameters are the same as in [12].

3. Results and discussion

In this section, we discuss the dynamics of blue InGaN tandem laser in terms of bifurcation diagrams. The calculations were carried out with the software package AUTO97 [14] for continuation and bifurcation problems of ordinary differential equations. The case when two currents are injected into regions A and B, both regions are active, is studied in more detail in [12]. Figure 2 shows the dependence of the photon number S on the injected current into region A for switch K in position 2 (Fig. 2a) and in position 3 (Fig. 2b). These characteristics show the threshold current of 60 mA for both cases. If switch K is in position 2, as shown in Fig. 2a, only the CW operation can be observed. Figure 2b shows a typical calculation of bifurcation for the periodic solution when switch K is in position 3. This figure shows the dependence of the peak of the photon number on the injected current. If we increase the injected current, the CW operation is observed (thin solid line) just after the threshold current. Then the laser begins to produce pulsations (thick solid line) through a Hopf bifurcation marked by a circle in Fig. 2b. A unique branch of stable self-pulsations exists in this region. Both Hopf points are supercritical.

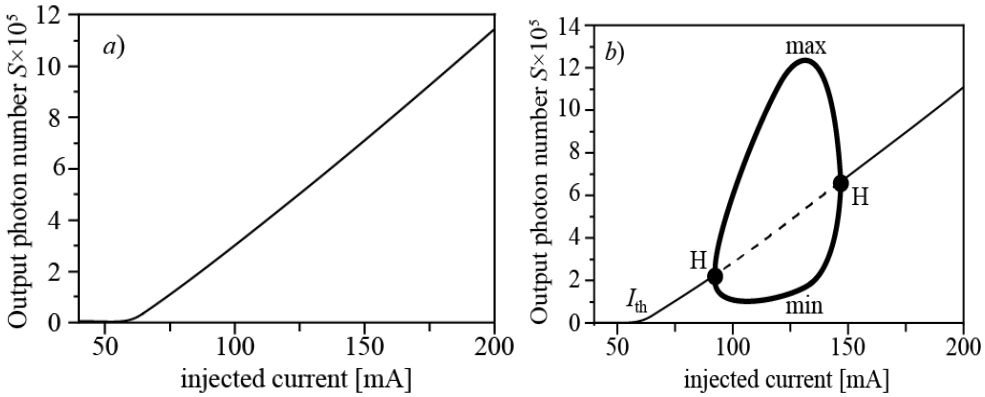

Fig. 2. Bifurcation diagram for switch K in position 2 (a) and in position 3 (b). Thin solid line: stable stationary (CW operation). Thin dotted line: unstable stationary states. Thick solid line: stable periodic solutions (self-pulsations). Further parameters: $\tau_{SA} = 1$ ns, $\tau_{SB} = 0.1$ ns, $n_{gA} = 2.3\times10^{25}$ m^{-3}, $n_{gB} = 0.1\times10^{25}$ m^{-3}, $a_A = 1.5\times10^{-12}$ m^{3}s^{-1}, $a_B = 9.0\times10^{-12}$ m^{3}s^{-1}.

If switch K is in position 3, for a 120-mA injected current, self-pulsation can be achieved with a frequency of 6.4 GHz. Figure 3 illustrates a typical time trace (left) and the power spectrum (right) of a tandem semiconductor laser in the self-pulsation regime. It can be observed that switch K in position 3 makes the laser structure produce stable self-pulsations. This self-pulsation has been experimentally confirmed in [12].

Next, we examine the effect of device and material parameters on the laser dynamics. Figure 4 shows calculated curves for regions of the self-pulsation where the injected current is

considered to be the bifurcation parameter. First, we discuss the possible variations of the cavity length in region B and injected current in region A. The solid line in Fig. 4a gives the boundary between the CW and non-lasing and the self-pulsation regions in the plane of these two parameters. If the cavity length in region B is smaller than 50 μm, the laser shows the CW or non-lasing operations. We mention that this criterion is valid if the other parameters are fixed as in Fig. 2b. An increase in the cavity length of region B leads to a wide self-pulsation region. However, this enlargement requires high injected currents (see Fig. 4a). On the other hand, a large carrier lifetime in the active region provides the appearance of self-pulsations for a lower injected current (see Fig. 4b). The appearance of self-pulsation strongly depends on diffusion time τ_T. Figure 4c shows the region of self-pulsation in the plane of diffusion time-injected current. The region of self-pulsation becomes wide for lower values of diffusion time.

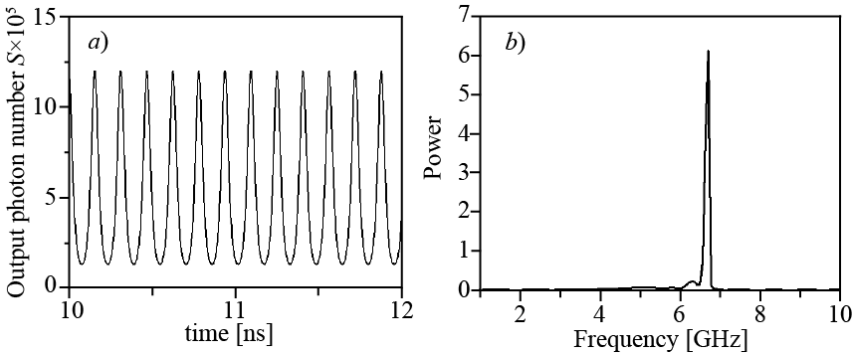

Fig. 3. Developing self-pulsation of the photon number (a) and power spectra (b) for the case of switch K in position 3 and a 120-mA injected current in region A. The parameters are the same as in Fig. 2b.

To estimate the self-pulsation frequency, the numerical simulations were carried out in the plane of different parameters. The results are plotted in Fig. 5, where the collared regions are the self-pulsating regions and the white region corresponds to the CW operation or non-lasing operation. It can be seen how the self-pulsation frequency changes in the plane of these parameters. The following features can be observed:

1. For a higher cavity length in region B, the region of self-pulsation is wide.
2. An increase in the differential gain coefficient in the active region A leads to a narrow SP region. However, the SP appears for a lower injected current.
3. The pulsation frequency becomes higher for a shorter carrier lifetime in region B and longer carrier lifetime in region A.

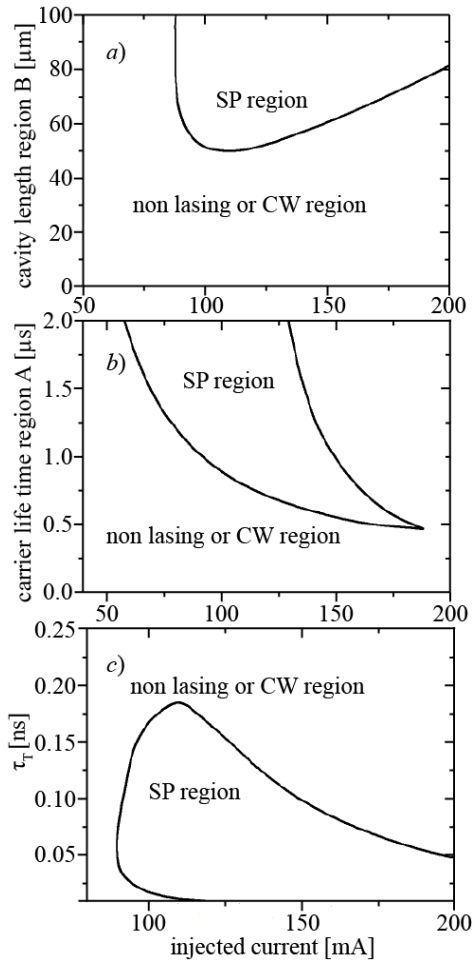

Fig. 4. SP regions in the plane of different parameters: (a) cavity length of region B versus injected current, (b) carrier lifetime in region A versus injected current, and (c) diffusion time versus injected current. The other parameters are the same as in Fig. 2b.

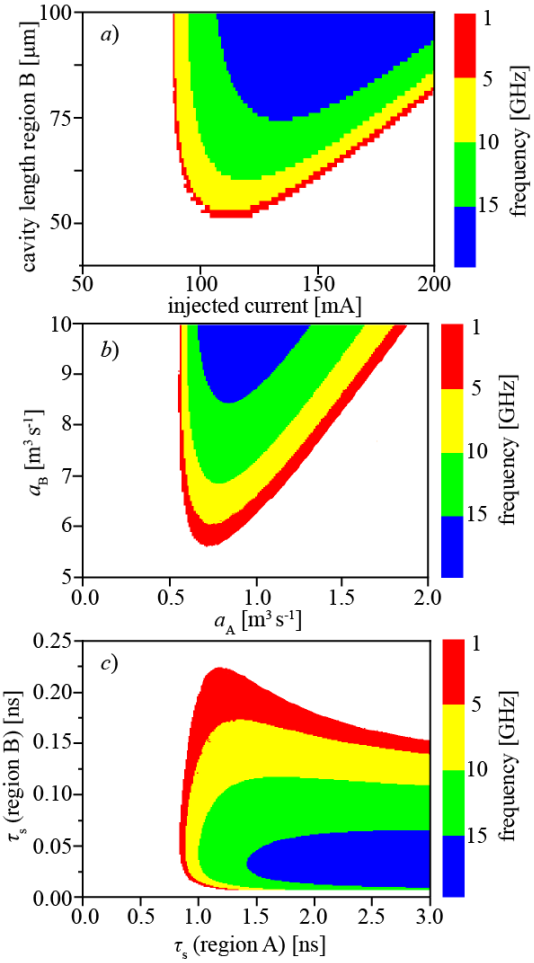

Fig. 5. Variation of frequency of self-pulsations in the plane of different parameters. The darkened regions are the self-pulsation regions. The white region corresponds to the CW or non-lasing operations. The other parameters are the same as in Fig. 2b.

4. Conclusions

The theoretical research reported in this paper has established that the tandem InGaN laser section in combination with an external circuit are promising candidates for the generation of high-frequency self-pulsations. The conditions for self-pulsation have been determined by calculations based on a single mode rate equation model of the device. A bifurcation analysis shows that a Hopf bifurcation is responsible for the appearance of self-pulsation under suitable conditions. It has been shown that a relatively short carrier lifetime in the SA is required for self-pulsation, whereas a large one is more appropriate for excitable behavior. Self-pulsation in a range of 1 to 15 GHz has been obtained in the numerical calculations. We believe that our work provides a good basis for subsequent more detailed studies of the SP end excitability in lasers with active region InGaN quantum wells.

Acknowledgments. The authors acknowledge the support of the Technical University of Moldova, project 106 b/s -11.817.05.17F. VZT acknowledges the support from the CIM – Returning Experts Programme.

References

[1] For a review, see, S. Nakamura, S. Pearton, and G. Fasol, The Blue Laser Diode, second ed., Springer, Berlin (2000).
[2] http://blue-ray.com
[3] M. Kneissl, D. P. Bour, C. G. Van de Walle, L. T. Romano, J. E. Northrup, R. M. Wood, M. Teepe, and N. M. Johnson, Appl. Phys. Lett. 75, 581 (1999).
[4] S. Nagahama, T. Yanamoto, M. Sano, and T. Mukai, Jpn. J. Appl. Phys. 40, L785 (2001).
[5] Sh. Ito, Y. Yamasaki, S. Omi, K. Takatani, T. Kawakami, T. Ohno, M. Ishida, Y. Ueta, T. Yuasa, and M. Taneya, Phys. Status Solidi A 200, 131 (2003)
[6] M. Yamada, J. Appl. Phys. 79, 61 (1996).
[7] S. Matsui, H. Takiguchi, H. Hayashi, S. Yamamoto, S. Yano, and T. Hijikata, Appl. Phys. Lett. 43, 219 (1983).
[8] V. Z. Tronciu, M. Yamada, and R. A. Abram, Phys. Rev. E, 70, 026604 (1-6), (2004)
[9] V. Z. Tronciu, M. Yamada, and R. A. Abram, AIUB J. Sci. Eng. 4, 7 (2005).
[10] V. Z. Tronciu, M. Yamada, T. Ohno, Sh. Ito, T. Kawakami, and M. Taneya, Phys. Status Solidi C, 7, 2296 (2003).
[11] V. Z. Tronciu, M. Yamada, T. Ohno, Sh. Ito, T. Kawakami, and M. Taneya, IEEE J. Quantum Electron. 39, 1509 (2003).
[12] V. Z. Tronciu, M. Yamada, T. Kawakami, Sh. Ito, T. Ohno, M. Taneya, and R. A. Abram, Optics Comm. 235, 409 (2004).
[13] M. Yamada, IEEE J. Quantum Electron. 30, 1511 (1994).
[14] E. J. Doedel, A. R. Champneys, T. F. Fairgrieve, Y. A. Kuznetsov, B. Sandstede, and X. Wang, Auto97 continuation and bifurcation software for ordinary differential equations, 1997.